IL NUOVO CIMENTO Vol. 31 C, N. 5-6 Settembre-Dicembre 2008
DOI 10.1393/ncc/i2008-10329-x

A re-evaluation of surface layer turbulence from Antarctic data

F. Tampieri and A. Maurizi
CNR-ISAC - Bologna, Italy

(ricevuto il 15 Ottobre 2008; approvato il 22 Gennaio 2009; pubblicato online il 9 Aprile 2009)

Summary. — A data set of velocity and temperature variances measured in the surface layer over a glacier in Antarctica is analysed in terms of the Monin-Obukhov Similarity Theory. The presence of surface inhomogeneities, flow unsteadiness, and other uncontrolled disturbances affects the shape of the distribution of normalised variances for intervals of the stability parameter. The modal value of the distribution, instead of the mean, is used to estimate the numerical coefficients of the similarity functions to minimize the influence of the (positive) outliers on the estimates. The overall agreement of the present results with previuos investigations is good, and also the spread of the numerical values noted by different authors is confirmed. In particular the investigation points out the need to use a similarity function for the temperature variance which diverges in near neutral conditions, as the heat flux goes to zero, and the occurrence of a large stability region where the variances of velocity and temperature are characterised by a behaviour almost independent of the momentum flux.

PACS 47.27.nb – Boundary layer turbulence.
PACS 92.60.Fm – Boundary layer structure and processes.
PACS 92.60.hk – Convection, turbulence, and diffusion.

1. – Introduction

Turbulence in the atmospheric surface layer is typically far from the ideal conditions which are required for the strict application of available theoretical frames. It is well known that the Monin-Obukhov Similarity Theory (MOST) needs horizontally homogeneous and steady conditions to be applied. As a consequence, data obtained under such restrictive conditions have to be used to put the correct numerical values in the similarity functions. Thus, there is a generalized experimental effort to obtain data under controlled conditions and to refine analysis techniques in order to cope with the widest range of situations. This effort becomes critical in the stable boundary layers, as discussed for instance by Cuxart *et al.* [1] or by Poulos *et al.* [2].

Another approach consists of the investigation of the effects of non-ideal conditions on atmospheric turbulence features. Again referring to prototypical cases, a number of investigations have been performed on fluxes perturbed by topography, changes in surface

conditions, or the presence of canopies or randomly sparse obstacles: see, among many others [3-6]. Unsteadiness is also a source of undesired effects; it must be taken into account for instance in all the situations characterised by low wind conditions: see [7,8]. From the experimental point of view, this approach also requires specific instrumental set-ups and special efforts to obtain reliable information.

There are, hovewer, several data sets which are affected by perturbations out of experimental control. Most of these data are taken in order to give a climatological description of specific sites, useful for applications like local weather prediction, air traffic control, pollution assessment and modelling.

Such data cannot be used directly for verification of the theory and for novel evalutions of empirical constants. Hovewer, for a correct use of the data in applications, it is important to assess their consistency with the underlying theory, and to achieve at least a qualitative evaluation of effects due to non-ideal conditions. In other words, as far as the departure from ideal conditions is recognized to be a climatological feature of a specific site, it is suggested that data analysis should focus on the identification of an average behaviour, the comparison with previous studies, and the interpretation of the departures (at least, of the order of magnitude of such departures) in terms of local conditions.

The purpose of this paper is to discuss a wide set of Antarctic sonic anemometer data. The variances of the three components of velocity and of sonic temperature are derived from the measurements. Although taken on flat terrain, the data are affected by a number of influences that lead to a large scatter. After a short presentation of the experimental conditions in sect. **2**, and of the theoretical frame in sect. **3**, sect. **4** goes on to discuss the distribution of observations, define the representative values for ranges of stability, and investigate their dependence on stability. In sect. **5** some conclusions are drawn.

2. – Data

The data used here were collected during three Antarctic campaigns in the years 1993-94, 1994-95 and 1998-99 by Italian researchers in the area of the Nansen Ice Sheet, during the austral summer. The coordinates of the stations were 74° 41′ 58″ S, 163° 30′ 50″ E; 74° 52′ 30″ S, 163° 00′ 00″ E; 74° 51′ 01″ S, 163° 27′ 42″ E for the three campaigns, respectively. Detailed information about the sites, the instruments and the periods can be found, for instance, in [9-11]. A schematic map of the area is shown in fig. 1.

The present paper deals only with data taken over flat terrain. The sampling heights varied in the different campaigns, covering a range from 2 m up to 22 m. The observations sampled by Gill ultrasonic anemometers (sampling rate 20.8 Hz) are averaged over half hour periods and detrended. The total number of data (each one referring to a half-hour period) is about 12000.

Evaluations of moments for shorter periods (say 10 min) are not available, preventing the possibility to separate slow motions, like waves, from small-scale fluctuations (turbulence, in common words), under stable conditions. This superposition of different effects produces a larger scatter in the stable data, but does not hinder the overall behaviour of data as a function of stability, as will be evident from the discussion carried on in the next sections.

The data have been analysed, looking for consistency with similarity theory. Being interested in analysing heat flux forcing effects (namely, the dependence of the similarity

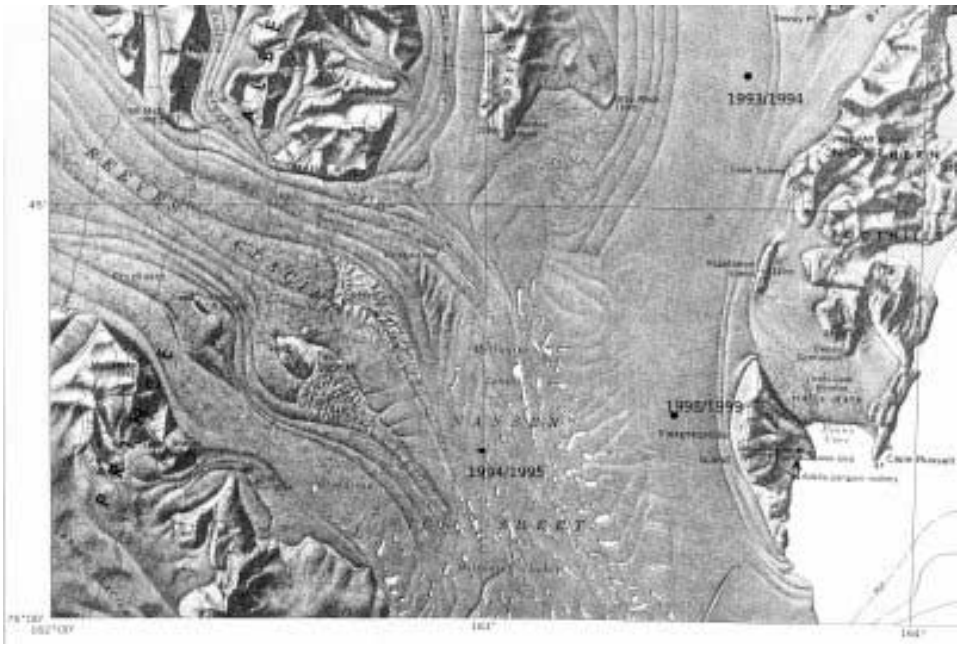

Fig. 1. – Map of the Nansen Ice Sheet. Approximate locations of the measurement sites, labelled with the years of the campaigns, are reported.

relations on the Obukhov length L_{MO}), a selection has been made based on the intensity of the sensible heat flux, excluding data with the absolute value of the kinematic heat flux below a threshold of $2 \times 10^{-3}\,\mathrm{K\,m\,s^{-1}}$.

3. – Theoretical remarks

The friction velocity is defined as

$$u_* = \left(\overline{u_1' u_3'}^2 + \overline{u_2' u_3'}^2\right)^{1/4}, \tag{1}$$

the temperature scale is

$$\vartheta_* = \overline{u_3' \vartheta'}/u_* \tag{2}$$

and the Obukhov length is

$$L_{MO} = -\frac{\vartheta_{00} u_*^3}{\kappa g \overline{u_3' \vartheta'}}, \tag{3}$$

where u_i' is the fluctuation in the i-th velocity component about the mean ($i = 1, 2, 3$ correspond to longitudinal, lateral and vertical direction), ϑ' the temperature fluctuation, ϑ_{00} is a reference temperature (here the mean temperature measured near the ground), $\kappa = 0.4$ is the von Karman constant and g the gravity acceleration. Sonic

temperature approximates virtual temperature, and is used here as temperature. Note that in the above definitions momentum and heat fluxes are assumed to be constant with height x_3.

The nondimensional 2nd-order similarity functions are defined as

$$\Phi_i(\zeta) = \frac{\overline{u_i'^2}}{u_*^2}\,, \tag{4}$$

$$\Phi_\vartheta(\zeta) = \frac{\overline{\vartheta'^2}}{\vartheta_*^2}\,, \tag{5}$$

where $\zeta = x_3/L_{MO}$ is the nondimensional height. This formulation holds in the surface layer, at heights x_3 much smaller than the boundary layer height h, and for horizontally homogeneous and steady conditions [12].

Functions Φ_i are expected to be independent of the momentum flux, and thus of u_*, in free-convection conditions [13], as the velocity scale reads, based on dimensional arguments,

$$w_*(x_3) = \left(\frac{g}{\vartheta_{00}}\overline{u_3'\vartheta'}|_0 x_3\right)^{1/3}. \tag{6}$$

Note that in this formulation the velocity scale is dependent on the height above the surface, and not on the convective boundary layer height. As clearly results from the literature and the present data, this velocity is the right scale for variances in the free-convective layer, giving $\overline{u_i'^2}/w_*(x_3)^2$ constant.

These functions are also assumed to take a constant value approaching neutrality, as u_* is the proper velocity scale.

Furthermore, the cited authors suggest that the transition from free convection to near-neutral conditions occurs within a layer (called dynamic-convective layer), in which the scales for horizontal and vertical velocity components are u_*^2/w_* and w_*, respectively. Performing the data analysis, a special care has been paid to look for the presence of this layer.

In moderately stable conditions, local values of the scales are of relevance, leading to the so-called z-less parameterisation [14,15], *i.e.* the variances are constant as normalised to the local flux values. Because the variances and the fluxes used here are taken at the same height, it is straighforward to refer to the parameterisation above. As far the local value of the momentum flux is effective in producing velocity fluctuations, the functions Φ_i are expected to be constant with stability.

In strong stability conditions, the turbulence fluctuations become less dependent on the momentum flux, the heat flux being the dominant mechanism acting on turbulence. Consistently, similarity functions are expected to become independent of u_* (see [16], p. 227), giving rise to a characteristic power law as a function of stability, although non-local effects like waves become of overwhelming importance.

A similar behaviour is expected of Φ_ϑ, with the notable exception of the neutral limit, because ϑ_* goes to zero and cannot be used as a proper scale for the ubiquitous albeit small fluctuations in temperature. Thus, in the neutral limit $\Phi_\vartheta \to \infty$.

The free-convection temperature scale is

$$\vartheta_{**} = \frac{\overline{u_3'\vartheta'}|_0}{w_*} \tag{7}$$

and applies in the same stability range as w_*.

The transition from free convection to near-neutral conditions (thus, the dynamic-convective layer) is characterized by the same temperature scale ϑ_*, according to Kader and Yaglom [13] but possibly by different numerical values of the coefficient of the fitting power law.

In moderately stable conditions, the correct temperature scale is still ϑ_*, so that the similarity function is constant with ζ: the fingerprint of the z-less parameterisation. In strong stability conditions the hypothesis of independence from u_* of the temperature variance leads the similarity function to be proportional to $\zeta^{-2/3}$.

Schematically, and neglecting the dynamic-convective layer in the unstable case:

- in the free-convection case ($-\zeta > \mathcal{O}(1)$): $\Phi_i \propto (-\zeta)^{2/3}$ and $\Phi_\vartheta \propto (-\zeta)^{-2/3}$;
- in near-neutral conditions ($|\zeta| \sim 0$): $\Phi_i \sim$ constant and $\Phi_\vartheta \sim |\zeta|^{-a}$, $a > 0$;
- in moderately stable conditions ($0 < \zeta < \mathcal{O}(1)$): both Φ_i and Φ_ϑ are constant, using local values of u_* and ϑ_*, namely, the values of the fluxes $\overline{u_i'u_3'}$, $i = 1, 2$ and $\overline{u_3'\vartheta'}$ measured at the anemometer height;
- in very stable conditions ($\zeta > \mathcal{O}(1)$): $\Phi_i \propto \zeta^{2/3}$ and $\Phi_\vartheta \propto \zeta^{-2/3}$.

In the present analysis, the dependence of the similarity functions on the boundary layer height has been neglected, because reliable estimates of such height are not available, and the measurement height is such that it can be estimated to lie in the surface layer in most cases.

4. – Data analysis

4˙1. *The data distribution.* – In the present theoretical frame, data analysis is performed investigating the dependence of the normalised variances on nondimensional height ζ. The data appear quite scattered, and a first step in the analysis is to determine the representative value for each range of ζ, for comparison with other data and for use in applications. An example is illustrated in fig. 2, that shows how the large scatter is not only due to small heat fluxes, but is probably related with other effects, like nonlocal disturbances and/or unsteadiness.

The scatter is found in many data sets and is due to the large number of uncontrolled factors, like horizontal inhomogeneity, unsteadiness, waves in stable cases, and low frequency disturbances. Because the variance is positively defined, the superposition of random disturbances produces a skewed distribution. Neglecting the physical origin of the disturbances, the distribution of data for classes of z/L_{MO} can be used as it is, in order to obtain a hint as to a representative value. The distribution of the logarithms of the normalised variances looks not far from Gaussian; accordingly, the distribution of the normalised variances is approximately log-normal, as can be seen in fig. 3.

The figure highlights the large asymmetry of the distribution. The distribution of any positively defined variable (such as the normalized variuances) is skewed, and the

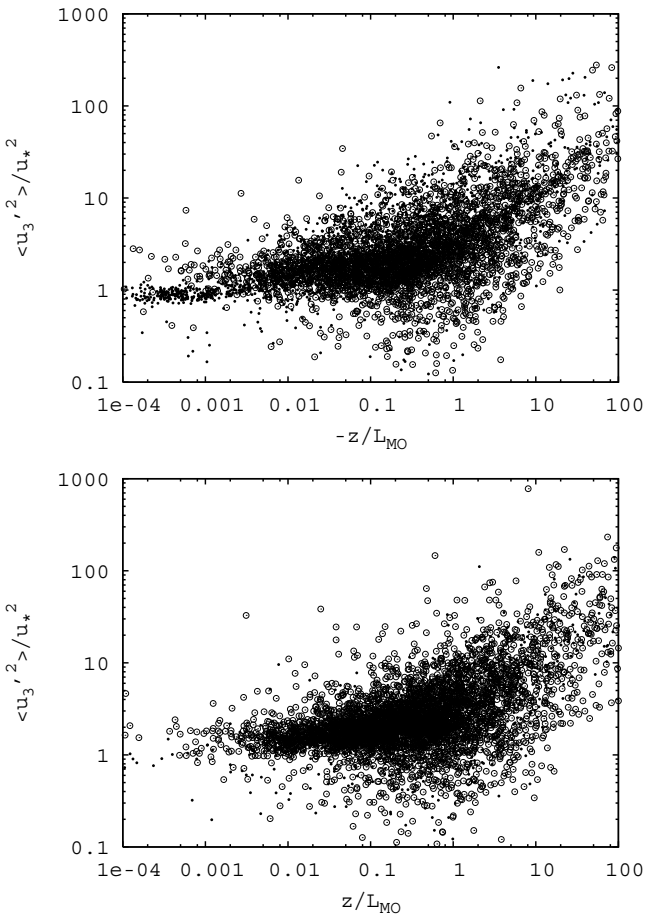

Fig. 2. – $\overline{u_3'^2}/u_*^2$ for unstable and stable conditions. Open circles refer to $|\overline{u_3'\vartheta'}| < 0.01\,\mathrm{K\,m\,s^{-1}}$, black dots otherwise. Note that in the axes of this figure and of the following ones, the averaged quantities are indicated with brackets istead of overline.

skewness is expected to be larger and larger as the variable is affected by uncontrolled errors. This means that the average value of the normalised variances is not representative of the data, being strongly affected by the long positive tail. By contrast, the median or even the mode may be considered estimates of the normalised variance, for each stability class, since they better reflect a value unaffected by non-local and/or unsteady disturbances. Note that the use of the mean value for estimating the similarity function is thus justified only if the spreading of the observations is quite small (standard deviation much smaller than the mean).

The median value for a log-normally distributed variable is given by $\exp[\mu]$; the mode is $\exp[\mu - \sigma^2]$ and the mean value is $\exp[\mu + \sigma^2/2]$, where μ is the mean of the Gaussian distributed logarithms of the same variable and σ^2 is the variance (see [17], p. 180).

Remembering that the median is the value of the variable that divides the total frequency into two equal halves, in the following analysis it will be adopted as a representative value for each z/L_{MO} range. In practice, the value is computed from the mean value of the logarithms of the normalised variances.

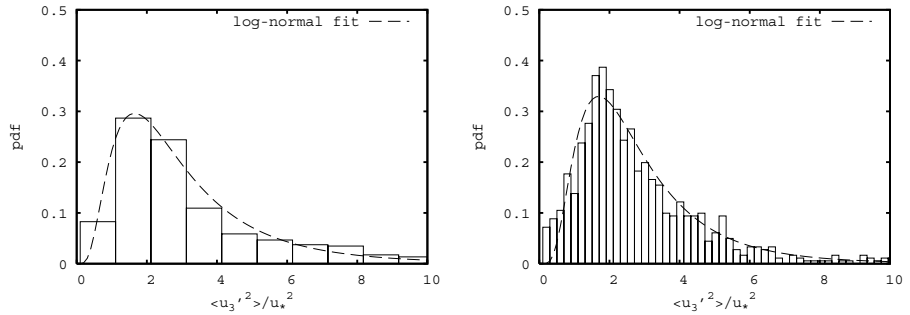

Fig. 3. – Normalised distribution of $\overline{u_3'^2}/u_*^2$ in the range $0.03 < |z/L_{MO}| < 0.1$ for unstable (left) and stable (right) conditions and the best-fit log-normal distribution. The width of the bins is different for stable and unstable cases, in order to have almost the same number of data in the most populated bins.

4˙2. *Dependence on stability.* – The medians for normalised variance of velocity components and temperature are plotted in figs. 4 to 7, together with some reference similarity functions from the literature. To compute the medians, logarithmically equally spaced bins have been used. The following functional forms for Φ are also fitted to the data:

– For velocity variances, and in all stability conditions:

$$\Phi_i = a_i + b_i|\zeta|^{2/3}, \quad i = 1, 2, 3. \tag{8}$$

– For temperature variance, in conditions from weak unstable to free convective (say, for $-\zeta > 0.01$, according to the present data):

$$\Phi_\vartheta = \frac{a_\vartheta}{1 + b_\vartheta(-\zeta)^{2/3}} \tag{9}$$

and in conditions from weak instability towards neutrality (for $0 < -\zeta < 0.01$):

$$\Phi_\vartheta = c(-\zeta)^{-2}. \tag{10}$$

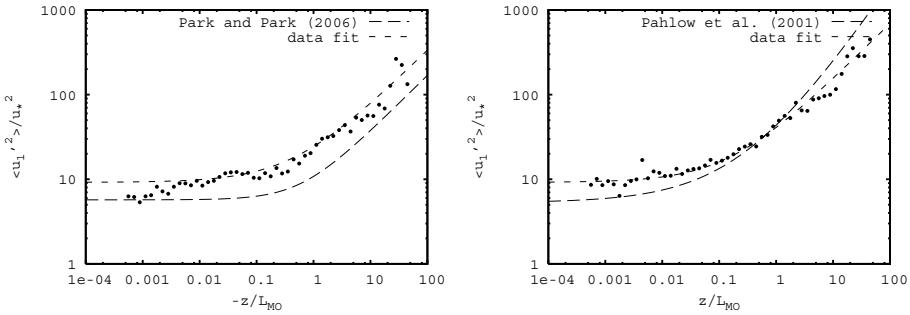

Fig. 4. – $\overline{u_1'^2}/u_*^2$ as a function of z/L_{MO} for unstable and stable conditions.

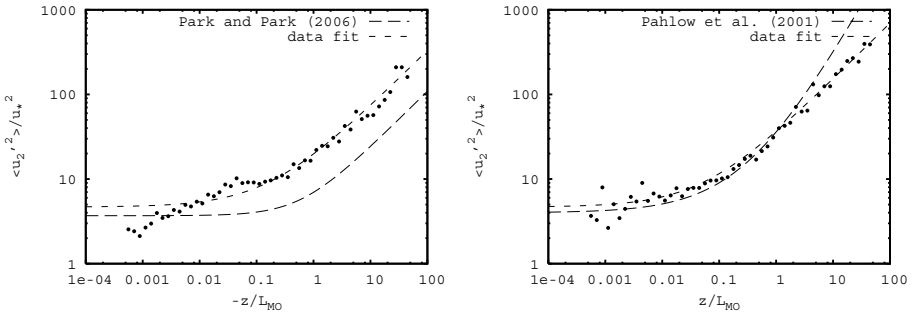

Fig. 5. – $\overline{u_2'^2}/u_*^2$ as a function of z/L_{MO} for unstable and stable conditions.

– For temperature variance, in weakly stable conditions (for $0 < \zeta < 1$):

$$\Phi_\vartheta = a_\vartheta + c\zeta^{-2} \tag{11}$$

and in strongly stable conditions (for $\zeta > 1$):

$$\Phi_\vartheta = b_\vartheta \zeta^{-2/3}. \tag{12}$$

As far the normalised velocity variance is concerned, eq. (8) is consistent with a constant value in near-neutral conditions (showing that u_* is the correct velocity scale), with the free-convection scaling (in this case $w_*(x_3)$ is the correct scale) and with the u_*-less scaling in strongly stable conditions.

The normalised temperature variance displays a bit more complex behaviour. The free-convection and u_*-less scalings are described by (9) and (12), for large $|\zeta|$. The divergence in near-neutral conditions, induced by the fact that the temperature scale ϑ_* goes to zero, is described by eqs. (10) and (11). Moreover, eq. (11) accounts also for the almost constant normalised variance (the z-less parameterisation) in moderately stable conditions.

The values of the coefficients obtained from fitting the above functions to the present data are reported in table I. Equation (8) has been forced to the same value of a_i, both

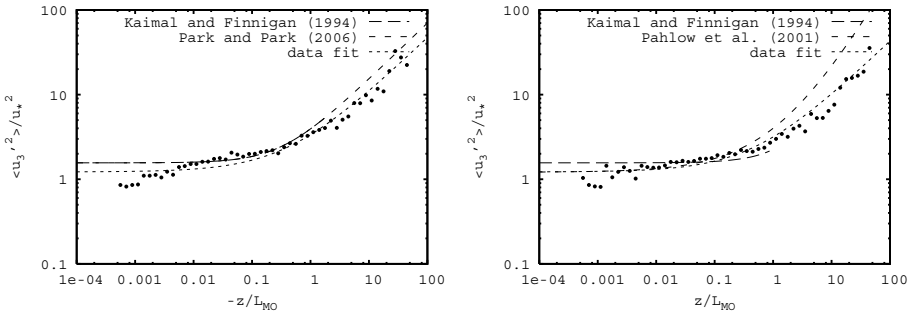

Fig. 6. – $\overline{u_3'^2}/u_*^2$ as a function of z/L_{MO} for unstable and stable conditions.

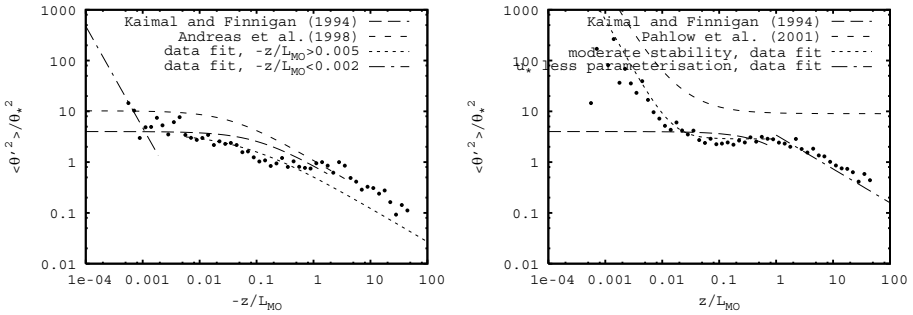

Fig. 7. – $\overline{\vartheta'^2}/\vartheta_*^2$ as a function of z/L_{MO} for unstable and stable conditions.

for unstable and stable conditions, determined from the median value for near-neutral conditions ($|\zeta| < 0.01$). For the temperature variance in stable conditions, the fit with eq. (11) is forced to take the constant value in the central stability range.

For comparison, some similarity expressions from recent literature are reported in figs. 4 to 7. For unstable conditions, the forms given by Park and Park [18] and Andreas *et al.* [3] are reported, for velocity components and temperature, respectively. For stable conditions, the forms given by Pahlow *et al.* [19] are shown. Moreover, the classical expressions for the vertical component of velocity and temperature by Kaimal and Finnigan [20] are reported.

In the convective cases, some functions from Kader and Yaglom [13] are also considered, in order to investigate the possibility of distinguishing between the dynamic-convective and free-convective sublayers. For the horizontal velocity components the theory suggests a different slope (*i.e.* $\zeta^{-2/3}$) with respect to the free-convective layer, but in the cited paper no evaluation of the coefficient is given. For the vertical component of velocity and temperature, the theory suggests the same slope for both the layers, possibly with different numerical coefficients. The dynamic-convective layer is expected to occur for $0.1 < -\zeta < 1$ (order of magnitude).

TABLE I. – *Coefficients from the data fit.*

Eq. (8)	a_i	b_i, unstable	b_i, stable
$i = 1$	9.2	13.7	29
$i = 2$	4.7	14.4	31.9
$i = 3$	1.2	1.97	1.69
Eq. (9)	a_ϑ	b_ϑ	
	3.7	6	
Eq. (10)	c		
	5×10^{-6}		
Eq. (11)	a_ϑ	c	
	2.8	7.5×10^{-5}	
Eq. (12)	b_ϑ		
	3.5		

The data are consistent with the picture given in sect. **3**, with the notable exception of the approach to neutral conditions, where no constant value is apparently reached, as far as velocity is concerned. The literature functions reported show that the numerical values of the constants, and thus the measured variances, may be quite different from one data set to another.

It seems impossible to justify quantitatively the existence of a dynamic-convective layer distinguishable from the free-convective one. However, changes in slope (for horizontal components) and in the numerical coefficient of the power law (for vertical component and temperature) for stability parameter around 0.1, suggest that this distinction should be further investigated.

In the strong stability range the data display slopes consistent with the u_*-less parameterisation. Previous works documented the increase of the normalised velocity variances with stability, using different (empirical) values for the power law. The increase of the normalised velocity variances implies that the scale velocity u_* decreases at least with the same power law, because the turbulent kinetic energy (*i.e.* the dimensional variances) is expected to decrease as stability increases.

In the stable layer, the local value of the momentum flux decreases with height above the ground, and as stability increases, the boundary layer height is expected to decrease. Because u_* is determined at the anemometer height, the decrease of boundary layer height leads to a decrease in the momentum flux measured by the anemometer. Whereas in the moderately stable case the z-less parameterisation affirms that the variance decreases with height at the same rate as the momentum flux (see [21]), so that the normalised variance is constant, both observations and the u_*-less parameterisation suggest that in very stable conditions the variance decreases at a rate slower than that of the momentum flux. In other words, some velocity variance still exists, although the friction velocity is quite small.

5. – Conclusions

The median values as functions of stability for normalised variances of velocity components and temperature derived from Antarctic observations over flat ice are shown to broadly agree with the standard MOST theory, including the u_*-less parameterisation for very stable conditions, displaying the expected slopes. The use of the median instead of the mean is justified by the skewness of the distribution of data. Although the present set looks affected by a number of undesired effects (like non-local disturbances, which are not filtered in the analysis) as far the stable boundary layer is concerned, this is not the case in convective cases. Thus the choice of the median should be considered as a useful tool in the analysis of variance data.

Compared with the literature determinations, it appears that there is substantial agreement among the present data and some authors, but there are also important differences.

At first, it can be observed that in very stable conditions the power law dependences suggested by Pahlow *et al.* [19] for velocity variance disagree with the present data, which are nearer to the 2/3 slope and agree with the predictions of the u_*-less parameterisation. The disagreement arises from the choice made by Pahlow *et al.* [19] to fit the data with a free exponent, instead of using a power law with fixed exponent.

In general, disagreement between different data sets has been considered as an index of the non-universality of the coefficients in the similarity functions derived in the frame

of MOST: this specific point has been addressed recently by Wilson [22] (see also the references herein).

However, the same disagreement may be used to stimulate deeper insight, if the basic equations are considered universal (this approach was explicitly cited by Cava *et al.* [23] in the specific case of the anomalous behaviour of the similarity functions for water vapour and carbon oxide concentrations with respect to that of temperature). If the values of the coefficients in the similarity functions vary from site to site, this can be interpreted as a variability of conditions which are out of control to the experimental set.

As an example of this point of view, let us consider the normalised temperature variance. The present data appear in general to be smaller than the published ones, especially in the stable case. The temperature fluctuations are related to the presence of small-scale inhomogeneity of the surface temperature, as noted by Kader and Yaglom [13]. The presence of a uniform iced surface reduces such inhomogeneities drastically, leading to the present result. To support this statement, it can be noted that in the present dataset about 35% of the standard deviation data is smaller than 0.2 K, whereas in a rural site near Rome (Italy) only 20% of data is below the said threshold. Although a more detailed investigation of this point is out of the scope of this paper, it is suggested as a topic for future investigations.

* * *

Scientific discussions with M. Tagliazucca led to substantial improvement of the work. The financial support by PNRA (National Programme for Antarctic Research) and by the Italia-USA Cooperation Agreement for Research on Climate Changes is gratefully acknowledged.

REFERENCES

[1] Cuxart J., Yague C., Morales G., Terradella E., Orbe J., Calvo J., Fernandez A., Soler M. R., Infante C., Buenestado P., Espinalt A., Joergensen H. E., Rees J. M., Vila J., Redondo J. M., Cantalapiedra I. R. and Conangla L., *Boundary-Layer Meteorol.*, **96** (2000) 337.
[2] Poulos G. S., Blumen W., Fritts D. C., Lundquist J. K., Sun J., Burns S. P., Nappo C., Banta R. M., Newson R. K., Cuxart J., Terradella E., Balsley B. B. and Jensen M., *Bull. Am. Meteorol. Soc.*, **83** (2002) 555.
[3] Andreas E. L., Hill R. J. and Gosz J. R., *Boundary-Layer Meteorol.*, **86** (1998) 379.
[4] Mammarella I., Tampieri F., Tagliazucca M. and Nardino M., *Environ. Fluid Mech.*, **5** (2005) 227.
[5] Moraes O. L. L., Acevedo O. C., Degrazia G. A., Anfossi D., da Silva R. and Anabor V., *Atmos. Environ.*, **39** (2005) 3103.
[6] Li W., Hiyama T. and Kobayashi N., *Boundary-Layer Meteorol.*, **124** (2007) 449.
[7] Mahrt L., *Boundary-Layer Meteorol.*, **125** (2007) 245.
[8] Mahrt L., *Boundary-Layer Meteorol.*, **127** (2008) 1.
[9] Giostra U., Cava D., Cardillo F. and Tagliazucca M., *Some characteristics of turbulence from summertime measurements over an Antarctic ice sheet*, in *Proceedings of 6th Workshop Italian Research on Antarctic Atmosphere*, edited by Colacino M., Giovanelli G. and Stefanutti L., Vol. **51** (Italian Physical Society, Bologna) 1996, pp. 25-38.
[10] Cava D., Giostra U., Trombetti F. and Tagliazucca M., *Spectral characteristics of waves and turbulence in a stable boundary layer*, in *Proceedings of 7th Workshop Italian Research on Antarctic Atmosphere*, edited by Colacino M., Giovanelli G. and Stefanutti L., Vol. **62** (Italian Physical Society, Bologna) 1998, pp. 167-179.

[11] Bortoli D., Cava D., Georgiadis T., Giostra U., Lavagnini A., Malvestuto V., Nardino M., Orsi G., Sempreviva A. M., Tagliazucca M., Transerici C. and Trivellone G., *Preliminary results from an experiment on the interaction of a flow with an orographic relief*, in *Proceedings of 8th Workshop Italian Research on Antarctic Atmosphere*, edited by Colacino M. and Giovanelli G., Vol. **69** (Italian Physical Society, Bologna) 2000, pp. 203-218.
[12] Monin A. S. and Yaglom A. M., *Statistical Fluid Mechanics*, Vol. **I** (MIT Press, Cambridge) 1971.
[13] Kader B. A. and Yaglom A. M., *J. Fluid Mech.*, **212** (1990) 637.
[14] Wyngaard J. C. and Coté O. R., *Q. J. R. Meteorol. Soc.*, **98** (1972) 590.
[15] Nieuwstadt F. T. M., *A model for the stationary, stable boundary layer*, in *Proceedings of Turbulence and Diffusion in Stable Environments*, edited by Hunt J. C. R. (Clarendon Press, Oxford) 1985, pp. 149-220.
[16] Grachev A. A., Fairall C. W., Persson P. O. G., Andreas E. L. and Guest P. S., *Boundary-Layer Meteorol.*, **116** (2005) 201.
[17] Kendall S. M. and Stuart A., *The Advanced Theory of Statistics*, Vol. **1** (C. Griffin & Co., London) 1977, 4th edition.
[18] Park M. S. and Park S. U., *Boundary-Layer Meteorol.*, **118** (2006) 613.
[19] Pahlow M., Parlange M. B. and Porte-Agel F., *Boundary-Layer Meteorol.*, **99** (2001) 225.
[20] Kaimal J. C. and Finnigan J. J., *Atmospheric Boundary Layer Flows. Their Structure and Measurement* (Oxford University Press) 1994.
[21] Nieuwstadt F. T. M., *J. Atmos. Sci.*, **41** (1984) 2202.
[22] Wilson J. D., *Boundary-Layer Meteorol.*, **129** (2008) 353.
[23] Cava D., Katul G., Sempreviva A. M., Giostra U. and Scrimieri A., *Boundary-Layer Meteorol.*, **128** (2008) 33.